



Group design in group testing for COVID-19: A French case-study

Tifaout Almeftah, Luce Brotcorne, Diego Cattaruzza, Bernard Fortz, Kaba Keita, Martine Labbé, Maxime Ogier, Frédéric Semet

► To cite this version:

Tifaout Almeftah, Luce Brotcorne, Diego Cattaruzza, Bernard Fortz, Kaba Keita, et al.. Group design in group testing for COVID-19: A French case-study. [Research Report] INRIA - Centre Lille Nord Europe. 2020. hal-03000715

HAL Id: hal-03000715

<https://inria.hal.science/hal-03000715>

Submitted on 12 Nov 2020

HAL is a multi-disciplinary open access archive for the deposit and dissemination of scientific research documents, whether they are published or not. The documents may come from teaching and research institutions in France or abroad, or from public or private research centers.

L'archive ouverte pluridisciplinaire **HAL**, est destinée au dépôt et à la diffusion de documents scientifiques de niveau recherche, publiés ou non, émanant des établissements d'enseignement et de recherche français ou étrangers, des laboratoires publics ou privés.

Group design in group testing for COVID-19 : A French case-study.

Tifaout Almeftah¹, Luce Brotcorne¹, Diego Cattaruzza², Bernard Fortz^{3,1}, Kaba Keita¹,
Martine Labbé^{3,1}, Maxime Ogier², and Frédéric Semet²

¹Inria Centre de recherche Lille Nord Europe, INOCS, F-59000 Lille, France

²Université de Lille, CNRS, Centrale Lille, Inria, UMR 9189 - CRISTAL, F-59000 Lille,
France

³Department of Computer Science, Université libre de Bruxelles, 1050 Brussels, Belgium

November 4, 2020

Abstract

Group testing is a screening strategy that involves dividing a population into several disjointed groups of subjects. In its simplest implementation, each group is tested with a single test in the first phase, while in the second phase only subjects in positive groups, if any, need to be tested again individually. In this paper, we address the problem of group testing design, which aims to determine a partition into groups of a finite population in such a way that cardinality constraints on the size of each group and a constraint on the expected total number of tests are satisfied while minimizing a linear combination of the expected number of false negative and false positive classifications. First, we show that the properties and model introduced by Aprahmian et al. can be extended to the group test design problem, which is then modeled as a constrained shortest path problem on a specific graph. We design and implement an ad hoc algorithm to solve this problem. On instances based on Santé Publique France data on Covid-19 screening tests, the results of the computational experiments are very promising.

Keywords— COVID-19; Group testing; Group design; Constrained shortest path; Dynamic programming.

1 Introduction

As COVID-19 has considerably impacted public health, some countries have privileged herd (collective) immunity, whereas many countries have undergone national lockdowns, which has significantly threatened the world economically and socially. By the end of spring 2020, when the spread and mortality rate of Covid-19 appeared to be under control, several countries have lifted lockdowns while respecting various measures (e.g., social distancing, wearing masks) to revive the economy of the nation and the education of youth.

The fact that the after lockdown has known an exploding number of infected cases and disease clusters is proving to be very worrying. Indeed, a second epidemic peak may force countries to decide on a local or general containment and, consequently, have an impact on all economic and social sectors trying to recover.

It is clear that no one can be spared from the virus. A significant number of patients can carry the virus without realizing it. They may be asymptomatic or pre-symptomatic, so they naturally continue to live their normal lives and are not isolated in the meantime. An increase in the number of undetected asymptomatic persons leads to an exponential increase in coronavirus spread, making the threat more

serious. Therefore, detecting massively daily Covid-19 carriers in the population is an urgent necessity to slow the uncontrollable spread of the virus.

The operation of screening a population of individuals to detect the infected subjects and the non-infected ones can rapidly consume huge resources (time, effort, money). The need for rapid test results is very important to reduce laboratory congestion, identify positive individuals, isolate them, and provide appropriate treatment when necessary. Moreover, it allows to better distinguish true negatives (who may feel some symptoms from other viral infections similar to those of Covid-19) and allow them to continue their daily social and economic activities. Therefore, massive tests are very important to screen the whole population. However, we cannot lower the classification quality, as it would let false negatives in the population and favor the spread of the virus.

From an economic point of view, a single Real-Time Polymerase Chain Reactor (RT-PCR) test, including the two steps of collecting individuals swab specimens and using pricey sophisticated equipment, can rapidly reach an approximate cost of 74 euros for the french Social Security, which leads to 300 millions euros per month.

Last, massive testing means more congestion in laboratories. There is a crucial need to reduce as much possible the stress felt by medical crews in laboratories and the costs of testing protocols.

Thus, reducing the cost and the social impact of classifying the population into two sets appears important. One strategy is to test samples of the population instead of testing each person individually, consequently saving scarce resources while maintaining the classification accuracy.

Dorfman initially introduced this method in 1943 [1] as Group Testing (GT). The principle of GT in its basic implementation is to divide the population into several disjoint groups of subjects, and, in the first stage, test each group with a single test. In the second stage, only subjects in positive groups, if any, need to be tested again individually. When the risk of being infected is low, especially with large scale populations, GT can be a highly beneficial strategy to screen all the subjects with minimal costs. In the case of a pandemic as Covid-19, the subjects to test can be pooled in groups where their samples are mixed and then tested with only one test. If viral RNA is not detected in the mixed samples, no one in the group is infected. Otherwise, at least one subject of the group is positive. In this case, a second phase of testing is fundamental to test every subject's sample individually to screen the infected patients.

Dorfman's scheme considers several theoretical assumptions as perfect tests, an infinite population, and the homogeneity of risk in the population that may not appear in real life. Indeed, the sensibility and the sensitivity of the tests play a major role in the possibility of having subjects classified as false-negative and false-positive. In reality, as the probability of being infected with Covid-19 cannot be the same for all subjects, we have to consider a heterogeneous population where individuals have different risks, which leads us to use the risk-based GT approach introduced in [2].

Specifically, our work is based on the following assumptions:

1. the tests are imperfect (with classification errors) and can be used on an individual sample as well as on a mixture of samples ;
2. the population to be screened, which is finite, includes subjects with different known probabilities of being Covid-19 positive, i.e. the prevalence of the disease varies within the population.

In this paper, we address the GT design problem (GTDP). The GTDP consists of determining a partition into groups of a finite population such that the cardinality of each group does not exceed a maximum value and that a testing budget constraint (i.e., representing the required number of tests to screen the population) is satisfied while minimizing a linear combination of the expected number of false negative and false positive classifications. The constraint on maximum group size plays a key role in the context of Covid-19 diagnosis as it avoids the dilution effect, which leads to a decrease in test sensibility. Indeed, the dilution of a single positive sample in a mixture of a large number of negative samples may likely make the positive sample undetectable, which may eventually cause misclassifications of some subjects. Our main contribution concerns the design, implementation, and evaluation of an exact optimization algorithm to determine such a partition of a population to be tested.

The remainder of the paper is organized as follows.. Section 2 presents a literature review. In Section 3, we describe the GT design problem and the notation used. The details on the algorithms proposed to tackle the GT problem are described in Section 4. Computational results are reported in Section 5. Finally, in Section 6, we draw conclusions and discuss future work.

2 Literature review

Since the pioneering work of Dorfman [1] in GT in 1943, several relevant scientific contributions were proposed to improve both the GT procedure and its application to various fields. In the following, we present some relevant contributions in the literature that deal with the GT design problem.

The well-known Dorfman’s GT procedure is based on two stages: in the first stage, subjects are tested in groups; if a group tests negative, then all subjects in the group are classified as negative; in the second stage, only subjects that belonged to positive groups are re-tested, one-by-one, to single out positives. Dorfman’s GT scheme suppose that the test is perfect, subjects are homogeneous, and the population to be tested is infinite. Several contributions in the literature based on this procedure can be found (see e.g., [3], [4], [5], [6], [7]). Later some contributions are proposed to extend Dorfman’s GT procedure. Hwang [4] proposes the earliest works to incorporate subject-specific risk characteristics in GT design. The extension to the realistic case of imperfect tests is introduced by [8], [9], [10], [11], [12]. The recent work proposed by Aprahamian et al. [2] relaxed all the unrealistic assumptions introduced initially in Dorfman’s GT procedure. However, they did not take into account the limitation on group size in all their experiments, although this limitation is relevant in some practical situations, as in the case of COVID-19.

GT has been largely used in several areas other than health, with applications considered in quality control ([3]), communications ([13], [14]), pattern matching ([15], [16]), database systems ([17]), traitor tracing ([18]), or machine learning ([19]). However, in the field of health care, the application of GT is the most widespread. The relevant applications include blood screening to detect human immunodeficiency virus (HIV), the detection of hepatitis B virus (HBV), and other diseases ([20], [21], [22], [23]), the screening of chemical compounds as part of the drug discovery ([24]), DNA screening ([25], [26], [27]).

Recently, some contributions have been proposed on the application of GT for Covid-19 screening. The prevalence rate of this disease being low with many asymptomatic cases, the application of GT is of great interest. Early works in the context of Covid-19 disease focused on determining the ideal group size beyond which the dilution effect causes false negatives. Yelin et al. [28] show that one can always detect a positive case in the mixed sample of a group of 32 or even 64 subjects under certain conditions. Ben-Ami et al. [29] suggest that the ideal group size should be eight subjects to ensure a reliable group test. Other contributions focused on the application of the GT scheme but using mainly statistical methods. Curturi et al. [30] propose noisy adaptive GT using Bayesian sequential experimental design with possible application in Covid-19 context. Ghosh et al. [31] present Tapestry: a single-round smart pooling technique for Covid-19 testing. The authors claim that Tapestry pooling gives confirmed results in a single round of testing by testing each sample thrice as part of three different pools.

Shental et al. [32] propose a GT scheme where they pooled 384 patient samples into 48 pools, each containing 48 samples. Each sample was added to six different pools. However, the number of groups and their size are not determined by an optimization algorithm.

In this paper, we propose a GT scheme applied to Covid-19 screening using advanced techniques derived from combinatorial optimization. We consider an imperfect test, a finite population and heterogeneous subjects as in [2]. Our main contribution is the addition of a limit on group size to avoid the dilution effect.

3 Problem definition and notation

This section relies on the work proposed by Aprahamian et al. [2]. Let $\mathcal{S} = \{\mathcal{S}_1, \dots, \mathcal{S}_N\}$ be the set of subjects to be tested. The risk vector, denoted $\mathbf{p} = (p^1, p^2, \dots, p^N)$, represents the probability of each individual of being infected by Covid-19. We assume subjects are ordered by increasing values of this risk, i.e. $p^1 \leq p^2 \leq \dots \leq p^N$.

The GTDP consists of finding an *optimal feasible* partition of set \mathcal{S} . As diagnostic tests are not error-free, we say that a partition is *optimal* if it minimizes a convex combination of expected false-negatives and expected false-positives tests. We say that a partition is *feasible* if it respects the cardinality constraint for each group, and the budget constraint. We denote by Se the test Sensitivity (i.e., true-positive probability) and by Sp the test Specificity (i.e., true-negative probability). With this notation, we can formulate the GT design problem as follows:

$$\begin{aligned}
& \underset{\Omega \in \mathbf{\Omega}}{\text{minimize}} && \lambda \mathbb{E}[FN(\Omega)] + (1 - \lambda) \mathbb{E}[FP(\Omega)] \\
& \text{subject to} && n_i \leq L \quad \forall i = 1, \dots, |\Omega|, \\
& && \mathbb{E}[T(\Omega)] \leq B,
\end{aligned} \tag{1}$$

where

- $\mathbf{\Omega}$ represents the set of all possible partitions of set \mathcal{S} ;
- Ω represents a single partition of set \mathcal{S} , and $|\Omega|$ represents the cardinality of the partition;
- n_i denotes the size of group Ω_i where $\Omega_i \in \Omega$ states that Ω_i is a set belonging to partition Ω ;
- $\mathbb{E}[FN(\Omega)]$ is the expected number of false-negative classifications;
- $\mathbb{E}[FP(\Omega)]$ corresponds to the expected number of false-positive classifications;
- $\mathbb{E}[T(\Omega)]$ represents the expected number of tests to perform;
- $\lambda \in [0, 1]$ is a weight, set by the decision maker, that controls the importance of false negatives versus false positives in the objective function;
- L is the maximum group cardinality;
- B is the test budget, i.e., the maximal number of tests that can be performed.

The objective function in model (1) minimizes the weighted sum of the expected number of false-negative and false-positive classifications. The constraints state that the size of each group cannot exceed the maximum group size and that the expected number of tests must be smaller or equal than a given testing budget.

3.1 Expected number of false negatives, positives and tests

Let $m \in \{1, \dots, |\mathcal{S}|\}$. We denote by \mathcal{S}_m the subject corresponding to position m in \mathcal{S} . Let I^m denote the indicator random variable corresponding to the true-positive status of subject $\mathcal{S}_m \in \mathcal{S}$. For a partition $\Omega \in \mathbf{\Omega}$, let $FN^m(\Omega)$ and $FP^m(\Omega)$, denote the indicator random variables, respectively corresponding to the false-negative classification and false-positive classification of subject \mathcal{S}_m . Similarly, let $N_i^+(\Omega_i)$, $FN_i(\Omega_i)$ and $FP_i(\Omega_i)$ respectively denote the counterparts of these random variables for group $\Omega_i \in \Omega$, $\forall i = 1, \dots, |\Omega|$. Note that, for a partition Ω , Ω^I and Ω^G respectively correspond to the sets of subjects to be tested individually and in groups. The computation of the expected number of false negatives, positives and tests is presented in Sections 3.1.1–3.1.3.

3.1.1 Expected number of false negatives

In individual testing, a truly positive subject is falsely classified as negative if the test outcome is negative. In contrast, in GT, a truly positive subject is falsely classified as negative if (i) the group test outcome is negative, or (ii) the group test outcome is positive, and the subject's subsequent individual test outcome is negative. Then, given a partition Ω , for any subject $\mathcal{S}_m \in \mathcal{S}$ with risk p^m , we have:

$$\mathbb{E}[FN^m] = \mathbb{E}[FN^m | I^m = 1]P(I^m = 1) + \mathbb{E}[FN^m | I^m = 0]P(I^m = 0)$$

$$= \begin{cases} (1 - Se)p^m + 0, & \text{if } \mathcal{S}_m \in \Omega^I, \\ (Se(1 - Se) + (1 - Se))p^m + 0, & \text{if } \mathcal{S}_m \in \Omega^G, \end{cases}$$

$$\text{leading to: } \mathbb{E}[FN^m] = \begin{cases} (1 - Se)p^m, & \text{if } \mathcal{S}_m \in \Omega^I, \\ (1 - Se^2)p^m, & \text{if } \mathcal{S}_m \in \Omega^G. \end{cases}$$

Then, the expected number of false-negative classifications for group i is given by:

$$\mathbb{E}[FN_i(\Omega_i)] = \begin{cases} (1 - Se) \sum_{m \in \Omega_i} p^m, & \text{if } n_i = 1, \\ (1 - Se^2) \sum_{m \in \Omega_i} p^m, & \text{otherwise,} \end{cases}$$

and the expected number of false-negative classifications for all subjects in set \mathcal{S} is given by:

$$\mathbb{E}[FN(\Omega)] = (1 - Se) \sum_{m \in \Omega^I} p^m + (1 - Se^2) \sum_{m \in \Omega^G} p^m. \quad (2)$$

3.1.2 Expected number of false positives

In individual testing, a truly negative subject is falsely classified as positive if the test outcome is positive, whereas in GT, a truly negative subject is falsely classified as positive if the group test outcome is positive and the subject's subsequent individual test outcome is positive. Then, given a partition Ω , for any individually tested subject $\mathcal{S}_m \in \Omega^I$, we can write:

$$\begin{aligned} \mathbb{E}[FP^m] &= \mathbb{E}[FP^m | I^m = 1]P(I^m = 1) + \mathbb{E}[FP^m | I^m = 0]P(I^m = 0) \\ &= 0 + (1 - Sp)(1 - p^m), \end{aligned}$$

and for any subject $\mathcal{S}_m \in \Omega^G$ grouped in some set Ω_i such that $i \in \{1, \dots, |\Omega|\}$, $n_i > 1$ (i.e., $\mathcal{S}_m \in \Omega_i$), we have:

$$\begin{aligned} \mathbb{E}[FP^m] &= \mathbb{E}[FP^m | I^m = 1]P(I^m = 1) + \mathbb{E}[FP^m | I^m = 0]P(I^m = 0) \\ &= 0 + \left[(1 - Sp)^2 \prod_{k \in \Omega_i \setminus \{m\}} (1 - p^k) + Se(1 - Sp) \left(1 - \prod_{k \in \Omega_i \setminus \{m\}} (1 - p^k) \right) \right] (1 - p^m) \\ &= (1 - Sp) \left[Se - (Se + Sp - 1) \prod_{k \in \Omega_i \setminus \{m\}} (1 - p^k) \right] (1 - p^m) \\ &= (1 - Sp)Se(1 - p^m) - (1 - Sp)(Se + Sp - 1) \prod_{k \in \Omega_i} (1 - p^k), \end{aligned}$$

leading to:

$$\mathbb{E}[FP_i(\Omega_i)] = \begin{cases} (1 - Sp)(1 - p^m), & \text{if } \mathcal{S}_m \in \Omega^I, \\ (1 - Sp)Se(1 - p^m) - (1 - Sp)(Se + Sp - 1) \prod_{k \in \Omega_i} (1 - p^k), & \text{if } \mathcal{S}_m \in \Omega^G. \end{cases}$$

Then, the expected number of false-positive classifications for group Ω_i is given by:

$$\mathbb{E}[FP_i(\Omega_i)] = \begin{cases} (1 - Sp) \sum_{m \in \Omega_i} (1 - p^m), & \text{if } n_i = 1, \\ (1 - Sp)Se \sum_{m \in \Omega_i} (1 - p^m) - ni(1 - Sp)(Se + Sp - 1) \prod_{m \in \Omega_i} (1 - p^m), & \text{otherwise,} \end{cases} \quad (3)$$

and the expected number of false-positive classifications for all subjects in set \mathcal{S} is given by $\mathbb{E}[FP(\Omega)] = \sum_i \mathbb{E}[FP_i(\Omega_i)]$.

3.1.3 Expected number of tests

In individual testing, the number of tests per subject is always one. In GT, the number of tests depends on the outcome of the group test: if the group test outcome is negative, then only one test is performed for the entire group, and if the group test outcome is positive, an additional individual test is performed for each subject in the group. Given a partition Ω , the expected number of tests for group Ω_i , $i = \{1, \dots, |\Omega|\}$, is 1 if $n_i = 1$ (i.e., individual testing), and if $n_i > 1$, we can write:

$$\begin{aligned} \mathbb{E}[T_i(\Omega_i)] &= \sum_{k=0}^{n_i} \mathbb{E}[T_i(\Omega_i) | N_i^+(\Omega_i) = k]P(N_i^+(\Omega_i) = k) \\ &= \mathbb{E}[T_i(\Omega_i) | N_i^+(\Omega_i) = 0]P(N_i^+(\Omega_i) = 0) \\ &\quad + \sum_{k=1}^{n_i} \mathbb{E}[T_i(\Omega_i) | N_i^+(\Omega_i) = k]P(N_i^+(\Omega_i) = k) \end{aligned}$$

$$\begin{aligned}
&= (Sp + (1 - Sp)(1 + n_i))P(N_i^+(\Omega_i) = 0) \\
&\quad + \sum_{k=1}^{n_i} (1 - Se + Se(1 + n_i))P(N_i^+(\Omega_i) = k) \\
&= 1 + n_i \left(Se - (Se + Sp - 1) \prod_{m \in \Omega_i} (1 - p^m) \right).
\end{aligned}$$

Thus,

$$\mathbb{E}[T_i(\Omega_i)] = \begin{cases} 1, & \text{if } n_i = 1, \\ 1 + n_i \left(Se - (Se + Sp - 1) \prod_{m \in \Omega_i} (1 - p^m) \right), & \text{otherwise,} \end{cases} \quad (4)$$

and the expected number of tests needed for all subjects in set \mathcal{S} is given by:

$$\mathbb{E}[T(\Omega)] = \sum_i \mathbb{E}[T_i(\Omega_i)].$$

For more details on how the expressions of the expected number of false negatives, positives and tests are computed, we refer the interested readers to [2].

4 An exact algorithm for the GTDP

Before presenting the algorithm that we develop to partition the sets of individuals in groups, let us introduce the definition of an *ordered partition* ([2]).

A partition, $\Omega = (\Omega_i)_{i=1, \dots, |\Omega|}$, is said to be an *ordered partition* if it follows the ordered set $\mathcal{S} = \{\mathcal{S}_1, \dots, \mathcal{S}_N\}$, that is, $\Omega_1 = \{\mathcal{S}_1, \dots, \mathcal{S}_{n_1}\}$, $\Omega_2 = \{\mathcal{S}_{n_1+1}, \dots, \mathcal{S}_{n_1+n_2}\}$, \dots , $\Omega_{|\Omega|} = \{\mathcal{S}_{\sum_{i=1}^{|\Omega|-1} n_i+1}, \dots, \mathcal{S}_N\}$, where $|\Omega| \in \{1, \dots, N\}$ and $n_i \in \mathbb{Z}^+$, $i = 1, \dots, |\Omega|$.

Aprahamian et al. [2] showed that the following properties hold for model (1) when only the maximum budget constraint is considered:

1. There exists an optimal partition that is an *ordered partition* of \mathcal{S} .
2. If subject \mathcal{S}_m is individually tested in an optimal partition, then it is optimal to individually test all subjects having a risk higher than p^m .

These properties remain valid when we consider the maximum group size constraints. Indeed, the proofs of both properties are based on the same type of argument. Let us consider the first property. Suppose that there exists an optimal partition Ω^* that does not follow an ordered partition of \mathcal{S} . Two groups of Ω^* violating the ordered partition property are identified. A new partition $\hat{\Omega}$ is then constructed by interchanging subjects between the two groups to satisfy the ordered partition property. All other groups of Ω^* remain unchanged in $\hat{\Omega}$. The key observation is that the subgroups of subjects interchanged between the two groups have the same cardinality in the proof by Aprahamian et al. [2]. This means that if Ω^* satisfies the cardinality constraints on the groups, $\hat{\Omega}$ also satisfies them. Therefore, the rest of the proof by Aprahamian et al. [2] is valid. The proof of the second property follows the same lines and is therefore valid when we impose the cardinality constraints on the size of the group.

Since the properties given above still hold, problem (1) reduces to solve a Constrained Shortest Path Problem [33] over the directed graph $G = (V, A)$ defined as follows:

- the node set $V = \mathcal{S} \cup \{\mathcal{S}_{N+1}\}$, contains one node per subject in \mathcal{S} , and an artificial node \mathcal{S}_{N+1} that represents a subject with risk 1;
- the arc set $A = \{(\mathcal{S}_i, \mathcal{S}_j) : \mathcal{S}_i, \mathcal{S}_j \in V, i < j, \mathbb{E}[T_i(\Omega_{i-j})] \leq B, j - i \leq L\}$, contains arcs $(\mathcal{S}_i, \mathcal{S}_j)$ that represent the corresponding groups $\Omega_{i-j} = \{\mathcal{S}_i, \mathcal{S}_{i+1}, \dots, \mathcal{S}_{j-1}\}$ that are feasible with respect to the maximum group size constraint and to the budget constraint;
- the cost of the arc $(\mathcal{S}_i, \mathcal{S}_j) \in A$ is equal to $C_{ij} = \lambda \mathbb{E}[FN_i(\Omega_{i-j})] + (1 - \lambda) \mathbb{E}[FP_i(\Omega_{i-j})]$.

Aprahamian et al. [2] showed that each path from node \mathcal{S}_1 to node \mathcal{S}_{N+1} corresponds to an ordered partition of set \mathcal{S} . To solve (1) as a Constrained Shorted Path Problem, we propose an algorithm derived from the exact algorithm of Feillet et al. [34], which is a dynamic programming based procedure based on a label correcting strategy. Due to the fact that the cost of the arcs of the graph $G = (V, A)$ are all positive, we do not have to impose elementarity reducing the complexity of the algorithm proposed in Feillet et al. [34]. Moreover, the acyclic structure of the graph helps in reducing the computational burden to obtain the optimal partition Ω of \mathcal{S} .

Paths and labels

Each feasible path between the sink (\mathcal{S}_1) and a node (\mathcal{S}_i) corresponds to a label l^i . Such a label is a triplet $l = (pred, C, R)$ containing a pointer to the label of its predecessor ($pred$) with respect to the order of subjects in the list \mathcal{S} , the cost of the path (C), and the consumption of the resource (R), which corresponds to the expected number of tests. We do not need to introduce an additional resource related to the size of the groups since groups that exceed the maximum size are excluded when constructing the graph.

Let l_1^i and l_2^i be two distinct paths from the sink (\mathcal{S}_1) to a node (\mathcal{S}_i). We say that $l_1^i < l_2^i$ (label l_1^i lower than l_2^i) if $C^{l_1^i} \leq C^{l_2^i}$. We store for every node (\mathcal{S}_i) in the acyclic graph the list of labels $\Lambda_i = \{l_1^i, l_2^i, \dots, l_k^i\}$ corresponding to all the possible paths from (\mathcal{S}_1) to (\mathcal{S}_i), with $l_1^i < l_2^i < \dots < l_k^i$.

Let \mathcal{S}_j ($j > 1$) be a node. Let $\mathcal{S}' = \{\mathcal{S}_i \in \mathcal{S} : i \in \{1, \dots, j-1\}\}$ be the list of predecessors of \mathcal{S}_j . Let Λ_i be the list of labels on every predecessor $\mathcal{S}_i \in \mathcal{S}'$. Each label l^j , corresponding to a feasible path from \mathcal{S}_1 to \mathcal{S}_j , is computed as follows :

For all label $l^i \in \Lambda_i$: $l^j = (l^i, C^{l^j}, R^{l^j})$ such as $C^{l^j} = C^{l^i} + C_{ij}$, $R^{l^j} = R^{l^i} + R_{ij}$ if $R^{l^j} + R_{ij} \leq B$ with $R_{ij} = \mathbb{E}[T_i(\Omega_{i-j})]$. For $j = 1$, there is no predecessors. Thus, Λ_1 contains only the label $(NIL, 0, 0)$.

As the number of labels on every node can increase exponentially, we only keep in memory the non dominated paths thanks to the following dominance rule.

Dominance rule

Let l_1^i and l_2^i be two distinct paths from the sink (\mathcal{S}_1) to a node (\mathcal{S}_i). l_1^i dominates l_2^i if and only if $l_1^i \leq l_2^i$ and $R^{l_1^i} \leq R^{l_2^i}$. This dominance rule allows us to save only Pareto-optimal paths all along the execution of the algorithm.

Algorithm

Algorithm **GTCSP** (GT Constrained Shortest Path Problem) is described in Algorithm 1. It applies the label correcting algorithm by traversing nodes in topological order on the implicit acyclic graph G . Thus, when processing a node \mathcal{S}_j , all the nodes $\mathcal{S}_i \in \{\mathcal{S} : i < j\}$ that precede it in topological order have their final labels. Labels of this node are, therefore, only computed once.

Starting by processing node \mathcal{S}_1 , at each step of the algorithm, the first unprocessed node in the topological order imposed by \mathcal{S} is selected. Then, all its labels are extended to each of its successors thanks to Algorithm 2 (**ExtendAndDominance**). Its outgoing arcs define the set of successors of a node.

Before inserting a label in the list of labels associated with the corresponding node, we check if the label is dominated by an already present label. In this case, the new label is discarded. If the new label is not dominated, we check if it dominates already present labels, and in the affirmative case, we discard the dominated labels.

To obtain the optimal partition after computing the shortest path with resource constraint between the first node and the artificial node, we browse the resulting path backward, as described in Algorithm 3.

Algorithm 1 GTCSPPhr/>**Input:**

- 1: - \mathcal{S} : ordered list of subjects of size N ,
- B : number of available tests.

Output: partition P of the subjects \mathcal{S}

```
2: function GTCSPPh( $\mathcal{S}, B, M$ )
3:   Add an artificial subject at the end of  $\mathcal{S}$  with  $risk = 1$ ;
4:    $\Lambda_1 \leftarrow (NIL, 0, 0)$ ;
5:   for  $j = 2, \dots, N + 1$  do
6:      $\Lambda_j \leftarrow \emptyset$ ;
7:      $i \leftarrow 1$ ;
8:     while  $(i < j)$  and  $((\mathcal{S}_i, \mathcal{S}_j) \in A)$  do
9:        $R_{ij} \leftarrow \mathbb{E}[T_i(\Omega_{i-j})]$ ;
10:       $C_{ij} \leftarrow \lambda \mathbb{E}[FN(\Omega_{i-j})] + (1 - \lambda) \mathbb{E}[FP(\Omega_{i-j})]$ ;
11:      for  $l \in \Lambda_i$  do
12:        if  $R^l + R_{ij} \leq B$  then
13:           $l' \leftarrow (l, C^l + C_{ij}, R^l + R_{ij})$ ;
14:           $\Lambda_j \leftarrow \text{ExtendAndDominance}(\Lambda_j, l)$ ;
15:        end if
16:      end for
17:       $i \leftarrow i + 1$ ;
18:    end while
19:  end for
20:  if  $\Lambda_{N+1} \neq \emptyset$  then
21:     $l \leftarrow \Lambda_{N+1}^1$ ;
22:     $I \leftarrow \emptyset$ ;
23:    while  $pred^l \neq NIL$  do
24:       $I \leftarrow I \cup \{pred^l\}$ ;
25:       $l \leftarrow pred^l$ ;
26:    end while
27:  end if
28:  Remove the artificial subject at the end of  $\mathcal{S}$ ;
29:   $P \leftarrow \text{RecoverPartition}(\mathcal{S}, I)$ ;
30:  return  $P$ ;
31: end function
```

Algorithm 2 Extend and dominance

Input:

- 1: - Λ_j : sorted list of size K of labels at a node j
- l : the new label to be added
- $\text{dominates}(l_1, l_2)$: returns *true* if $R^{l_1} \leq R^{l_2}$ when $l_1 < l_2$

Output: insert l in the right position in Λ_j if not dominated and remove dominated labels if

```
any
2: function EXTENDANDDOMINANCE( $\Lambda_j, l$ )
3:    $index \leftarrow 0$ ;
4:   if  $\Lambda_j = \emptyset$  then
5:      $index \leftarrow 0$ ;
6:   else
7:      $i \leftarrow 1$ ;
8:     while  $i \leq K$  do
9:       if  $l < \Lambda_j^i$  then
10:         $index \leftarrow i$ ;
11:        if  $\text{dominates}(l, \Lambda_j^i)$  then
12:          while  $i \leq K$  do;
13:            if  $\text{dominates}(l, \Lambda_j^i)$  then
14:              remove  $\Lambda_j^i$ ;
15:            else
16:               $i \leftarrow i + 1$ ;
17:            end if
18:          end while
19:        end if
20:        break;
21:      else
22:        if  $\text{dominates}(\Lambda_j^i, l)$  then
23:           $index \leftarrow 0$ ;
24:          break;
25:        else
26:           $index \leftarrow i$ ;
27:           $i \leftarrow i + 1$ ;
28:        end if
29:      end if
30:    end while
31:  end if
32:  if  $index \neq 0$  then
33:    insert  $l$  at  $index$  in  $\Lambda_j$ 
34:  end if
35:  return  $\Lambda_j$ ;
36: end function
```

Algorithm 3 Recover partition

Input:

- 1: - \mathcal{S} : list of subjects
- I : list of size M of labels corresponding to first elements in every group

Output: The corresponding partition P

```
2: function RECOVERPARTITION( $\mathcal{S}, I$ )
3:   for  $i = M, \dots, 1$  do
4:      $P \leftarrow P \cup \emptyset$ ;
5:     for  $j = I^i, \dots, I^{i-1}$  do
6:        $P^{M-i} \leftarrow P^{M-i} \cup \mathcal{S}_j$ ;
7:     end for
8:   end for
9:   return  $P$ ;
10: end function
```

Figure 1: An example of graph with 8 subjects, \mathcal{S}_9 is the artificial one.

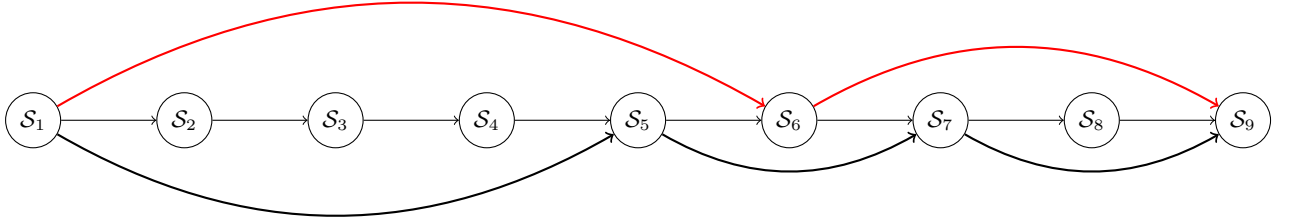


Figure 1 shows the graph $G = (V, A)$ corresponding to an example of 8 subjects $\mathcal{S} = \{\mathcal{S}_1, \mathcal{S}_2, \dots, \mathcal{S}_8\}$. Let $\mathbf{p} = \{0.01, 0.02, 0.03, 0.04, 0.05, 0.06, 0.07, 0.08\}$ be the corresponding risk vector.

The costs C_{ij} of the arcs $(\mathcal{S}_i, \mathcal{S}_j) \in A, i < j$, are computed as explained above. Let $Se = Sp = 0.75$, $\lambda = 0.6$ and $B = 6$. The optimal solution computed by Algorithm 1 is $\Omega^* = \{\{\mathcal{S}_1, \mathcal{S}_2, \mathcal{S}_3, \mathcal{S}_4, \mathcal{S}_5\}, \{\mathcal{S}_6, \mathcal{S}_7, \mathcal{S}_8\}\}$, with an expected cost $C = 0.311$ and an expected number of tests $R = 5.444$. The other depicted path corresponds to the feasible partition $\Omega = \{\{\mathcal{S}_1, \mathcal{S}_2, \mathcal{S}_3, \mathcal{S}_4\}, \{\mathcal{S}_5, \mathcal{S}_6\}, \{\mathcal{S}_7, \mathcal{S}_8\}\}$ with with an expected cost $C = 0.332$ and an expected number of tests $R = 4.647$.

5 Computational experiments

In this section, we evaluate the *GTCSPP* algorithm proposed to tackle the GTDP in the case of Covid-19 screening. We ran our algorithm on instances generated from the data-set provided by the French national health care agency (Santé publique France). We used data related to Covid-19 screening tests carried out in city laboratories. These data concern all 101 French departments. They cover 11 weeks, from week 11 to week 21 of 2020 (March 10 to May 24). This period corresponds to the peak of the first epidemic in France.

The data set contains the number of tests performed, **404,550**, the number of people tested, **404,046** and the number of people tested positive, **39,830**. These data are classified by gender (women and men) and by age group (five age groups). Table 1 and 2 report the numbers of women and men tested, the number of women and men tested positive, and the risk of Covid-19 for each subgroup.

5.1 Instance generation

An instance of the GTDP is composed of a set of subjects that must be tested. Each subject has a risk, i.e., Covid-19 prevalence rate. The prevalence of a disease corresponds to the number of cases in

Table 1: The number of women tested, the number of women tested positive and the risk of Covid-19 for each age group of women

Week			11	12	13	14	15	16	17	18	19	20	21
Age group													
Women under 15 years	pos		0	1	10	16	12	4	5	2	3	12	5
	tot		22	86	144	211	248	226	245	213	411	1004	1014
	risk		0	1.16	6.94	7.58	4.84	1.77	2.04	0.94	0.73	1.2	0.49
Women between 15-44 years	pos		44	573	1856	2047	1575	859	571	257	188	148	79
	tot		272	2798	8532	11958	12026	11788	11752	7951	9155	11355	8708
	risk		16.18	20.48	21.75	17.12	13.1	7.29	4.86	3.23	2.05	1.3	0.91
Women between 45-64 years	pos		43	525	1634	1896	1565	833	477	231	139	112	47
	tot		201	1841	6289	9395	10281	9938	9806	6798	7851	9582	7298
	risk		21.39	28.52	25.98	20.18	15.22	8.38	4.86	3.4	1.77	1.17	0.64
Women between 65-74 years	pos		11	117	366	390	351	221	117	42	48	32	24
	tot		37	328	1209	1753	2164	2089	2140	1440	1842	2801	2365
	risk		29.73	35.67	30.27	22.25	16.22	10.58	5.47	2.92	2.61	1.14	1.01
Women 75 years and over	pos		19	237	782	1307	2383	1656	965	337	281	268	141
	tot		71	824	2762	3917	9250	12581	12418	7928	7837	7266	4631
	risk		26.76	28.76	28.31	33.37	25.76	13.16	7.77	4.25	3.59	3.69	3.04

pos : number of positive women.
tot : total number of women tested.
risk : Covid-19 prevalence rate (%).

Table 2: The number of men tested, the number of men tested positive and the risk of Covid-19 for each age group of men

Week			11	12	13	14	15	16	17	18	19	20	21
Age group													
Men under 15 years	pos		3	10	25	41	21	13	18	11	8	21	9
	tot		24	103	171	208	204	246	268	216	387	1160	1161
	risk		12.5	9.71	14.62	19.71	10.29	5.28	6.72	5.09	2.07	1.81	0.78
Men between 15-44 years	pos		38	291	837	804	573	362	234	140	108	80	55
	tot		170	1066	3190	4655	4926	4552	4700	3543	4529	7449	5921
	risk		22.35	27.3	26.24	17.27	11.63	7.95	4.98	3.95	2.38	1.07	0.93
Men between 45-64 years	pos		32	399	1213	1119	760	416	265	124	98	85	45
	tot		119	1089	3530	4792	4846	4285	4599	3394	4200	6172	4933
	risk		26.89	36.64	34.36	23.35	15.68	9.71	5.76	3.65	2.33	1.38	0.91
Men between 65-74 years	pos		18	200	551	477	342	205	126	43	47	22	20
	tot		64	468	1501	1851	1918	1861	2030	1430	1713	2666	2259
	risk		28.13	42.74	36.71	25.77	17.83	11.02	6.21	3.01	2.74	0.83	0.89
Men 75 years and over	pos		13	192	654	784	874	526	310	133	93	87	55
	tot		54	625	1746	2282	3536	4225	4364	2960	2919	3291	2423
	risk		24.07	30.72	37.46	34.36	24.72	12.45	7.1	4.49	3.19	2.64	2.27

pos : number of positive men.
tot : total number of men tested.
risk : Covid-19 prevalence rate (%).

Table 3: χ^2 significance test of prevalence between different age groups of women

Age group \ Week	11	12	13	14	15	16	17	18	19	20	21
W-15 vs 4 others	green	green	green	green	green	green	green	green	green	red	red
W15-44 vs 3 others	red	green	green	green	green	green	red	red	red	red	red
W45-64 vs 2 others	red	red	green	red	red	green	red	green	green	red	red
W65-74 vs W75+	red	green	red	green	green	green	green	green	green	green	green

W-15, W15-44, W45-64, W65-74, W75+ : Women under 15, between 15-44, 45-64, 65-74 and 75 years and over.

4 others : W15-44, W45-64, W65-74, W75+.

3 others : W45-64, W65-74, W75+.

2 others : W65-74, W75+.

green week 11 : means W-15 has a prevalence of Covid-19 significantly different to the ones of all other age groups for the week 11 (see the first row).

red week 20 : means W-15 has a prevalence of Covid-19 that is not significantly different to at least one of the others for the week 20 (see the first row).

Table 4: χ^2 significance test of prevalence between different age groups of men

Age group \ Week	11	12	13	14	15	16	17	18	19	20	21
M-15 vs 4 others	red	green	green	red	red	red	red	red	red	red	red
M15-44 vs 3 others	red	red	green	green	green	green	red	red	red	red	red
M45-64 vs 2 others	red	green	red	green	green	red	red	red	red	green	red
M65-74 vs M75+	red	green	red	green	green	red	red	green	red	green	green

M-15, M15-44, M45-64, M65-74, M75+ : Male under 15, between 15-44, 45-64, 65-74 and 75 years and over.

4 others : M15-44, M45-64, M65-74, M75+.

3 others : M45-64, M65-74, M75+.

2 others : M65-74, M75+.

green week 18 : means M65-74 has a prevalence of Covid-19 significantly different to the one of M75+ for the week 18 (see the last row).

red week 11 : means M-15 has a prevalence of Covid-19 that is not significantly different to at least one of the others for the week 11 (see the first row).

a population at a given point in time, including both new and old cases. The risk of each subject is determined according to his/her gender age group. We compute each gender age group risk weekly (see Table 1 and 2) as Covid-19 prevalence vary along time. Note that the French national health care agency initially defined the partition of the data set into age groups by gender. To ensure that it is meaningful to use different risks by gender and age group, we need to verify whether the risks are statistically different by performing χ^2 tests on the data for the entire period of the epidemic. Results of statistical tests are reported in Tables 3, 4 and 5. These tables report the χ^2 test results on the significance of women, men, and women and men Covid-19 prevalences. Columns correspond to weeks of Covid-19 screening tests and rows report the comparisons between a gender age group prevalence and the other ones. A green cell in the table indicates that the prevalence of the gender-age group this week is significantly different from the prevalences of all other gender-age groups. A red cell indicates that the prevalence of the gender-age group is not significantly different from at least one of the other gender-age group prevalences. The results in Tables 3, 4 and 5 show that the prevalences of the 10 gender-age groups are not statistically different during the epidemic period in France. Therefore, we group the same age group of different genders, reducing the numbers of groups from 10 to 5. The partition of the number of people tested, the number of people tested positive and the risk of Covid-19 for each of the 5 age groups is reported in Table 6.

The χ^2 tests on the new partition of the population into 5 age groups show that from week 14 to

Table 5: χ^2 significance test of prevalence between different age groups of women and men

Age group \ Week	11	12	13	14	15	16	17	18	19	20	21
W-15 vs 5 others											
W15-44 vs 5 others											
W45-64 vs 5 others											
W65-74 vs 5 others											
W75+ vs 5 others											

W-15, W15-44, W45-64, W65-74, W75+ : Female under 15, between 15-44, 45-64, 65-74 and 75 years and over.

M-15, M15-44, M45-64, M65-74, M75+ : Male under 15, between 15-44, 45-64, 65-74 and 75 years and over.

5 others : M-15, M15-44, M45-64, M65-74, M75+.

green week 21 : means W75+ has a prevalence of Covid-19 significantly different to the ones of all the others for the week 21 (see the last row).

red week 11 : means M-15 has prevalence of Covid-19 that is not significantly different to at least one of the others for the week 11 (see the first row).

Table 6: The number of people tested, the number of people tested positive and the risk of Covid-19 for each age group

people age group \ Week		11	12	13	14	15	16	17	18	19	20	21
people under 15 years	pos	3	11	35	57	33	17	23	13	11	33	14
	tot	46	189	315	419	452	472	513	429	798	2164	2175
	risk	6.52	5.82	11.11	13.6	7.3	3.6	4.48	3.03	1.38	1.52	0.64
people between 15-44 years	pos	82	864	2693	2851	2148	1221	805	397	296	228	134
	tot	442	3864	11722	16613	16952	16340	16452	11494	13684	18804	14629
	risk	18.55	22.36	22.97	17.16	12.67	7.47	4.89	3.45	2.16	1.21	0.92
people between 45-64 years	pos	75	924	2847	3015	2325	1249	742	355	237	197	92
	tot	320	2930	9819	14187	15127	14223	14405	10192	12051	15754	12231
	risk	23.44	31.54	28.99	21.25	15.37	8.78	5.15	3.48	1.97	1.25	0.75
people between 65-74 years	pos	29	317	917	867	693	426	243	85	95	54	44
	tot	101	796	2710	3604	4082	3950	4170	2870	3555	5467	4624
	risk	28.71	39.82	33.84	24.06	16.98	10.78	5.83	2.96	2.67	0.99	0.95
people 75 years and over	pos	32	429	1436	2091	3257	2182	1275	470	374	355	196
	tot	125	1449	4508	6199	12786	16806	16782	10888	10756	10557	7054
	risk	25.6	29.61	31.85	33.73	25.47	12.98	7.6	4.32	3.48	3.36	2.78

pos : number of positive people.

tot : total number of people tested.

risk : Covid-19 prevalence rate (%).

Table 7: χ^2 significance test of prevalence between different age groups

Age group \ Week	11	12	13	14	15	16	17	18	19	20	21
-15 vs 4 others											
15-44 vs 3 others											
45-64 vs 2 others											
65-74 vs 75+											

-15, 15-44, 45-64, 65-74, +75 : People under 15, between 15-44, 45-64, 65-74 and 75 years and over.

4 others : 15-44, 45-64, 65-74, 75+.

3 others : 45-64, 65-74, 75+.

2 others : 65-74, 75+.

green week 21 : means people between 65-74 years have a prevalence of Covid-19 significantly different to the ones of 75 years and over people for the week 21 (see the last row).

red week 17 : means people under 15 years have a prevalence of Covid-19 that is not significantly different to at least one of the others for the week 17 (see the first row).

week 16 all the risks of the subgroup are statistically different two-by-two (see Table 7). This table has the same format as Tables 3, 4 and 5.

To generate an instance, we considered the daily data related to Covid-19 screening tests in the department of North in France. We disaggregated the data to obtain individual data. We assumed that the prevalences available on week W are those computed for week $W - 1$. Thus, we assigned to each subject the risk of the previous week $W - 1$ according to his/her age group. We obtained six instances representing one-day Covid-19 screening tests from week 14 to 16. They include 54, 54, 157, 146, 104 and 100 subjects tested on March 30 and 31, and April 8, 9, 14 and 17 respectively. As these instances are associated with different weeks, they present a certain diversity, which allows us to evaluate the effect of the size and composition of an instance on the optimal solution. The aggregated data of the six instances are presented in Tables 8 to 13. For each instance, we report the Covid-19 prevalence rate (risk), the total number of people tested and the number of positive ones by age group.

We set the test sensitivity of the RT-PCR tests Se to 0.7 and specificity Sp to 0.95. According to [35], these are conservative values from systematic reviews [36]. λ is set to 0.8 to favor the minimization of expected false negatives.

The testing budget B or the number of available tests to be conducted should clearly be at most $|\mathcal{S}| - 1$ to need partitioning \mathcal{S} , otherwise we test all the population individually. To tighten B , starting from $B = |\mathcal{S}| - 1$, we decrease the budget of available tests as much as we can until the algorithm fails to find a solution.

Note that another way to have an approximate value of B is to simply compute $B' = \mathbb{E}[T(\Omega_{1-(N+1)})]$ where $\Omega_{1-(N+1)} = \{\mathcal{S}_1, \mathcal{S}_2, \dots, \mathcal{S}_N\}$. B' can be used as starting value to decrease from instead of $B = |\mathcal{S}| - 1$.

5.2 Computational results

We present the results of our experiments on real instances arising from Covid-19 screening tests performed in laboratories in the Northern department of France. Results are computed with the procedure proposed in Section 4. The procedure is coded in C++ and experiments are run on an Intel® Core™ i7-9850H CPU @ 2.60GHz 2.59GHz computer with 16 Gb of RAM.

Researchers have shown the accuracy of GT when the size of groups does not exceed a specific number. Using the standard COVID-19 RT-qPCR test, [28] showed that a single positive subject can be detected in a pool of up to 32 persons, while [29] has shown the accuracy of limiting the group sizes to only eight subjects. We used both limits for the group size in our experiments.

The computational results on the six instances are reported in Tables 14 and 15. Each row in the tables is associated with one instance. In the first three columns, we indicate the number of subjects, the minimum and the maximum Covid-19 risk values. The fourth column reports the minimum number of tests needed. The optimal value of the weighted sum of the expected number of false-negative and false-

Table 8: **Instance 1:** 54 subjects resulting from Covid-19 screening tests on March 30, week 14, in city laboratories in the department of North in France. The risks are those of week 13 for the department of North.

Ages (years)	risk	Number	Positive
-15		0	0
15-44	0.238	18	1
45-64	0.339	18	5
65-74	0.370	4	2
75+	0.253	14	5
Total		54	13

Table 9: **Instance 2:** 54 subjects resulting from Covid-19 screening tests on March 31, week 14, in city laboratories in the department of North in France. The risks are those of week 13 for the department of North.

Ages (years)	risk	Number	Positive
-15		0	0
15-44	0.238	18	3
45-64	0.339	21	1
65-74	0.370	4	0
75+	0.253	11	7
Total		54	11

positive classifications is reported in the fifth column. The sixth column reports the number of groups formed. The seventh and eighth columns report the minimum and maximum numbers of subjects in a group. The ninth column shows the expected gain in percentage in terms of test budget compared with the individual screening solution. The last column reports the computation time in seconds.

When we compare the results for a group size fixed to 8 and 32 in Table 14, we notice that for all instances, the number of tests required found when the group size is fixed to 8 is greater or equal to that found when the group size is 32. Nevertheless, the group size of 8 tends to perform slightly better in terms of misclassification errors as measured by the objective function value (see column **objVal** in Table 14). A smaller objective function value corresponds to a higher test precision. However, when the population size increases, better results are obtained in terms of test budget and precision with a group size fixed to 32. For example, for Instance 3 with 157 subjects tested, the test budget and the test precision are 103 and 12.80 respectively when the group size is 32. These values are 104 and 12.91 respectively when the group size is 8.

The use of GT is always better than the current practice of testing each subject individually regardless of whether the group size is limited to 32 or 8. In our experiments on real instances, we can achieve more than 34% of expected gain compared to the current practice (see column **Gain** in Table 14). This expected gain depends on the size of the population and the prevalence rate of the disease. We will have a much higher gain if we consider a large population with a low prevalence rate.

Concerning the optimal solution, we observe that the minimum number of tests required (**B**), the misclassification errors (**objVal**), the number of groups formed (**G**), the groups lower-bound (**minSubG**) and upper-bound (**maxSubG**) depend on the size of the population and the subject risks in an instance. For example, Instance 1 and 2 have the same number of subjects. However, the test precision is different in the two cases (see Table 14).

In Table 15, we compare the results when the group size is fixed to 8 and 32 by setting the test budgets to the same value. We observe that a group size of 32 leads to better results in terms of misclassification errors with large instances (see column **objVal** in Table 15).

Table 10: **Instance 3:** 157 subjects resulting from Covid-19 screening tests on April 8, week 15, in city laboratories in the department of North in France. The risks are those of week 14 for the department of North.

Ages (years)	risk	Number	Positive
-15	0.000	2	0
15-44	0.187	76	14
45-64	0.152	44	6
65-74	0.125	13	5
75+	0.369	22	7
Total		157	32

Table 11: **Instance 4:** 146 subjects resulting from Covid-19 screening tests on April 9, week 15, in city laboratories in the department of North in France. The risks are those of week 14 for the department of North.

Ages (years)	risk	Number	Positive
-15	0.000	1	0
15-44	0.187	59	11
45-64	0.152	45	8
65-74	0.125	12	2
75+	0.369	29	7
Total		146	28

Table 12: **Instance 5:** 104 subjects resulting from Covid-19 screening tests on April 14, week 16, in city laboratories in the department of North in France. The risks are those of week 15 for the department of North.

Ages (years)	risk	Number	Positive
-15	0.000	3	1
15-44	0.157	49	9
45-64	0.199	34	9
65-74	0.176	4	0
75+	0.277	14	1
Total		104	20

Table 13: **Instance 6:** 100 subjects resulting from Covid-19 screening tests on April 17, week 16, in city laboratories in the department of North in France. The risks are those of week 13 for the department of North.

Ages (years)	risk	Number	Positive
-15	0.000	0	0
15-44	0.157	49	7
45-64	0.199	36	5
65-74	0.176	9	0
75+	0.277	6	1
Total		100	13

Table 14: Results over the 6 real instances with a limit of 8 vs 32 on the group size

Instances	nbSub	minRisk	maxRisk	B		objVal		G		minSubG		maxSubG		Expected Gain (%)		CPU (s)
				8	32	8	32	8	32	8	32	8	32	8	32	
Inst1	54	0.238	0.370	42	40	6.29	6.44	14	8	1	1	8	32	22.22	25.93	0.00
Inst2	54	0.238	0.370	42	40	6.46	6.54	13	8	1	1	8	32	22.22	25.93	0.00
Inst3	157	0.000	0.369	104	103	12.91	12.80	38	37	1	1	8	19	33.76	34.39	0.00
Inst4	146	0.000	0.369	98	96	12.66	12.66	34	32	1	1	8	28	32.88	34.25	0.00
Inst5	104	0.000	0.277	69	68	7.88	8.08	29	23	1	4	4	14	33.65	34.62	0.00
Inst6	100	0.000	0.277	66	66	7.58	7.58	26	26	1	1	5	5	34.0	34.0	0.00

nbSub: number of subjects in the instance

minRisk: minimum value of Covid-19 risk for the instance

maxRisk: maximum value of Covid-19 risk for the instance

B: the minimal number of available tests required to find a partition by the algorithm

objVal: objective function value

G: number of groups in the optimal solution

minSubG: minimal number of subjects in a group

maxSubG: maximal number of subjects in a group

CPU (s): CPU time in seconds

Expected Gain (%): expected gain in percentage compared to the individual screening solution

Table 15: Results over the 6 real instances with a limit of 8 vs 32 on the group size and the same budget

Instances	nbSub	minRisk	maxRisk	B		objVal		G		minSubG		maxSubG		Expected Gain (%)		CPU (s)
				8	32	8	32	8	32	8	32	8	32	8	32	
Inst1	54	0.238	0.370	42	42	6.29	6.00	14	14	1	1	8	29	22.22	22.22	0.00
Inst2	54	0.238	0.370	42	42	6.46	6.10	13	14	1	1	4	4	9.25	9.25	0.00
Inst3	157	0.000	0.369	104	104	12.91	12.62	38	40	1	1	8	16	33.76	33.76	0.00
Inst4	146	0.000	0.369	98	98	12.66	12.24	34	38	1	1	8	21	32.88	32.88	0.00
Inst5	104	0.000	0.277	69	69	7.88	7.88	29	29	1	1	4	4	33.65	33.65	0.00
Inst6	100	0.000	0.277	66	66	7.58	7.58	26	26	1	1	5	5	34.0	34.0	0.00

nbSub: number of subjects in the instance

minRisk: minimum value of Covid-19 risk for the instance

maxRisk: maximum value of Covid-19 risk for the instance

B: the minimal number of available tests required to find a partition by the algorithm

objVal: objective function value

G: number of groups in the optimal solution

minSubG: minimal number of subjects in a group

maxSubG: maximal number of subjects in a group

CPU (s): CPU time in seconds

Expected Gain (%): expected gain in percentage compared to the individual screening solution

6 Conclusions

GT is a screening strategy that can be very efficient to test samples of a large population instead of individual screening since it reduces the required resources while maintaining the classification accuracy. For a given maximum size of the groups to be identified, a key question is how to build such groups, which can be modeled as the Group Testing Design Problem (GTDP). In this paper, we extended the results of Aprahamian et al. [2] when we impose a maximum size for the groups. Then, the GTDP can still be modeled as a constrained shortest path problem, which can be solved in polynomial time due to the acyclic property of the underlying graph. Computational results on instances derived from data provided by Santé Publique France show that the proposed algorithm is able to provide solutions that reduce the number of tests by up to 34% compared with an individual screening strategy while minimizing a convex combination of the expected numbers of false-negative and false-positive classifications in very short computation times.

The main perspective of this work is to investigate how the results could be further improved by designing a more relevant segmentation of the population. The population is currently segmented according to age groups set by Santé Publique France, and the risks are calculated accordingly. We might benefit from designing a more relevant segmentation depending on the risks. Other relevant information, such as co-morbidities, could then be taken into account. Another perspective would be to consider additional constraints in the GTDP related to the technical characteristics of the clinical test, and to see how the properties, on which the approach is based, are still preserved.

References

- [1] R. Dorfman, The detection of defective members of large populations, *The Annals of Mathematical Statistics* 14 (4) (1943) 436–440.
- [2] H. Aprahamian, D. R. Bish, E. K. Bish, Optimal risk-based group testing, *Management Science* 65 (9) (2018) 4365–4384, <https://doi.org/10.1287/mnsc.2018.3138>.
- [3] M. Sobel, P. A. Groll, Group testing to eliminate efficiently all defectives in a binomial sample, *Bell System Technical Journal* 38 (5) (1959) 1179–1252.
- [4] F. K. Hwang, A generalized binomial group testing problem, *Journal of the American Statistical Association* 70 (352) (1975) 923–926.
- [5] B. A. Saraniti, Optimal pooled testing, *Health Care Management Science* 9 (2) (2006) 143–149.
- [6] J. Feng, L. Liu, M. Parlar, An efficient dynamic optimization method for sequential identification of group-testable items, *Mathematics IIE Transactions* 43 (2) (2010) 69–83.
- [7] T. Li, C. L. Chan, W. Huang, S. Jaggi, Group testing with prior statistics, *IEEE International Symposium on Information Theory* (2014) 2346–2350.
- [8] C. R. Bilder, J. M. Tebbs, Pooled-testing procedures for screening high volume clinical specimens in heterogeneous populations, *Statistics in Medicine* 31 (27) (2012) 3261–3268.
- [9] M. S. Black, C. R. Bilder, J. M. Tebbs, Group testing in heterogeneous populations by using halving algorithms, *Journal of Royal Statistical Society, Series C* 61 (2) (2012) 277–290.
- [10] C. S. McMahan, J. M. Tebbs, C. R. Bilder, Informative dorfman screening, *Biometrics* 68 (1) (2012) 287–296.
- [11] J. M. Tebbs, C. S. McMahan, C. R. Bilder, Informative dorfman screening, *Biometrics* 69 (4) (2013) 1064–1073.
- [12] M. S. Black, C. R. Bilder, J. M. Tebbs, Optimal retesting configurations for hierarchical group testing, *Journal of Royal Statistical Society, Series C* 64 (4) (2015) 693–710.
- [13] T. Berger, N. Mehravari, D. Towsley, J. Wolf, Random multiple-access communication and group testing, *IEEE Transactions on communications* 32 (7) (1984) 769–779.

- [14] J. Wolf, Born again group testing: Multiaccess communications, *IEEE Transactions on Information Theory* 31 (2) (1985) 185–191.
- [15] A. J. Macula, L. J. Popyack, A group testing method for finding patterns in data, *Discrete Applied Mathematics* 144 (1-2) (2004) 149–157.
- [16] R. Clifford, K. Efremenko, E. Porat, A. Rothschild, Pattern matching with don't cares and few errors, *Journal of Computer and System Science* 76 (2) (2010) 115–124.
- [17] G. Cormode, S. Muthukrishnan, What's hot and what's not: tracking most frequent items dynamically, *ACM Transactions on Database Systems* 30 (1) (2005) 249–278.
- [18] P. Meerwald, T. Furon, Group testing meets traitor tracing, *IEEE International Conference on Acoustics, Speech and Signal Processing (ICASSP)* (2011) 4204–4207.
- [19] Y. Zhou, U. Porwal, C. Zhang, H. Q. Ngo, X. Nguyen, C. Ré, V. Govindaraju, Parallel feature selection inspired by group testing, Vol. 27, Z. Ghahramani and M. Welling and C. Cortes and N.D. Lawrence and K.Q. Weinberger, 2014, pp. 3554–3562.
- [20] J. Gastwirth, W. Johnson, Screening with cost effective quality control: Potential applications to hiv and drug testing, *Journal of the American Statistical Association* 89 (427) (1994) 972–981.
- [21] S. K. Bar-Lev, O. Boxma, W. Stadje, F. A. V. der Duyn Schouten, Screening with cost effective quality control: Potential applications to hiv and drug testing, *Methodology and Computing in Applied Probability* 12 (2010) 309–322.
- [22] C. R. Blider, J. M. Tebbs, P. Chen, Informative retesting, *Journal of the American Statistical Association* 105 (491) (2010) 942–955.
- [23] S. L. Stramer, U. Wend, D. Candotti, G. A. Foster, F. B. Hollinger, R. Y. Dodd, J. P. Allain, W. Gerlich, Nucleic acid testing to detect hbv infection in blood donors, *The New England Journal of Medicine* 364 (3) (2011) 236–247.
- [24] L. Zhu, J. M. Hughes-Oliver, S. S. Young, Statistical decoding of potent pools based on chemical structure, *Biometrics* 57 (3) (2001) 922–930.
- [25] A. J. Macula, Probabilistic nonadaptive group testing in the presence of errors and dna library screening, *Annals of Combinatorics* 3 (1999) 61–69.
- [26] D. Du, F. K. Hwang, Pooling designs and nonadaptive group testing, in: W. Scientific (Ed.), *Important Tools for DNA Sequencing*, Vol. 18 of *Applied Mathematics*, 2006, p. 248.
- [27] C. Cao, X. Sun, Combinatorial pooled sequencing: experiment design and decoding, *Quantitative Biology* 4 (2016) 36–46.
- [28] I. Yelin, N. Aharony, E. S. Tamar, A. Argoetti, E. Messer, D. Berenbaum, E. Shafran, A. Kuzli, N. Gandali, O. Shkedi, T. Hashimshony, Y. Mandel-Gutfreund, M. Halberthal, Y. Geffen, M. Szwarcwort-Cohen, R. Kishony, Evaluation of covid-19 rt-qpcr test in multi-sample pools, *Clinical Infection Diseases* (2020).
- [29] R. Ben-Ami, A. Klochendler, M. Seidel, T. Sido, O. Gurel-Gurevich, M. Yassour, E. Meshorer, G. Benedek, I. Fogel, E. Oiknine-Djian, A. Gertler, Z. Rotstein, B. Lavi, Y. Dor, D. Wolf, M. Salton, Y. Drier, Large-scale implementation of pooled rna extraction and rt-pcr for sars-cov-2 detection, *Clinical Microbiology and Infection* 26 (2020) 1248–1253.
- [30] M. Cuturi, O. Teboul, Q. Berthet, A. Doucet, J. Vert, Noisy adaptive group testing using bayesian sequential experimental design, <https://arxiv.org/abs/2004.12508> (2020).
- [31] S. Ghosh, A. Rajwade, S. Krishna, N. Gopalkrishnan, T. E. Schaus, A. Chakravarthy, S. Varahan, V. Appu, R. Ramakrishnan, S. Ch, M. Jindal, V. Bhupathi, A. Gupta, A. Jain, R. Agarwal, S. Pathak, M. A. Rehan, S. Consul, Y. Gupta, N. Gupta, P. Agarwal, R. Goyal, V. Sagar, U. Ramakrishnan, S. Krishna, P. Yin, D. Palakodeti, M. Gopalkrishnan, Tapestry: A single-round smart pooling technique for covid-19 testing, <https://doi.org/10.1101/2020.04.23.20077727> (2020).

- [32] N. Shental, S. Levy, S. Skorniakov, V. Wuvshet, Y. Shemer-Avni, A. Porgador, T. Hertz, Efficient high throughput sars-cov-2 testing to detect asymptomatic carriers, <https://doi.org/10.1101/2020.04.14.20064618> (2020).
- [33] R. Garcia, Resource constrained shortest paths and extensions, Ph.D. thesis, Georgia Institute of Technology (2009).
- [34] D. Feillet, P. Dejax, M. Gendreau, C. Gueguen, An exact algorithm for the elementary shortest path problem with resource constraints: Application to some vehicle routing problems, *Networks* 44 (3) (2004) 216–229.
- [35] J. Watson, P. F. Whiting, J. E. Brush, Interpreting a covid-19 test result, *BMJ* 369 (2020). arXiv:<https://www.bmj.com/content/369/bmj.m1808.full.pdf>, doi:10.1136/bmj.m1808. URL <https://www.bmj.com/content/369/bmj.m1808>
- [36] I. Arevalo-Rodriguez, D. Buitrago-Garcia, D. Simancas-Racines, P. Zambrano-Achig, R. del Campo, A. Ciapponi, O. Sued, L. Martinez-Garcia, A. Rutjes, N. Low, et al., False-negative results of initial rt-pcr assays for covid-19: a systematic review, *medRxiv* (2020).